Published OnlineFirst May 24, 2018; DOI: 10.1158/1078-0432.CCR-17-3348

Clinical Trials: Targeted Therapy

Clinical Cancer Research

# Phase 0 Trial of AZD1775 in First-Recurrence Glioblastoma Patients

Nader Sanai[1], Jing Li[2], Julie Boerner[2], Karri Stark[2], Jianmei Wu[2], Seongho Kim[2], Alanna Derogatis[1], Shwetal Mehta[1], Harshil D. Dhruv[3], Lance K. Heilbrun[2], Michael E. Berens[3], and Patricia M. LoRusso[4]

## Abstract

**Purpose:** AZD1775 is a first-in-class Wee1 inhibitor with dual function as a DNA damage sensitizer and cytotoxic agent. A phase I study of AZD1775 for solid tumors suggested activity against brain tumors, but a preclinical study indicated minimal blood–brain barrier penetration in mice. To resolve this controversy, we examined the pharmacokinetics and pharmacodynamics of AZD1775 in patients with first-recurrence, glioblastoma.

**Patients and Methods:** Twenty adult patients received a single dose of AZD1775 prior to tumor resection and enrolled in either a dose-escalation arm or a time-escalation arm. Sparse pharmacokinetic blood samples were collected, and contrast-enhancing tumor samples were collected intraoperatively. AZD1775 total and unbound concentrations were determined by a validated LC/MS-MS method. Population pharmacokinetic analysis was performed to characterize AZD1775 plasma pharmacokinetic profiles. Pharmacodynamic endpoints were compared to matched archival tissue.

**Results:** The AZD1775 plasma concentration–time profile following a single oral dose in patients with glioblastoma was well-described by a one-compartment model. Glomerular filtration rate was identified as a significant covariate on AZD1775 apparent clearance. AZD1775 showed good brain tumor penetration, with a median unbound tumor-to-plasma concentration ratio of 3.2, and achieved potential pharmacologically active tumor concentrations. Wee1 pathway suppression was inferred by abrogation of $G_2$ arrest, intensified double-strand DNA breakage, and programmed cell death. No drug-related adverse events were associated with this study.

**Conclusions:** In contrast to recent preclinical data, our phase 0 study of AZD 1775 in recurrent glioblastoma indicates good human brain tumor penetration, provides the first evidence of clinical biological activity in human glioblastoma, and confirms the utility of phase 0 trials as part of an accelerated paradigm for drug development in patients with glioma. *Clin Cancer Res; 24(16); 3820–8. ©2018 AACR.*

*See related commentary by Vogelbaum, p. 3790*

## Introduction

Glioblastoma is the most frequently reported malignant brain tumor histology (29.6%) in the National Cancer Database. The prognosis for these patients is bleak, with the median survival after diagnosis ranging from 12 to 16 months (1, 2). Although conventional treatment with a combination of surgery, irradiation, and temozolomide postpones tumor progression and extends patients' survival, these tumors universally recur and unrelentingly result in patient death.

Despite their own genetic aberrations, glioblastoma cells still must maintain a functional genome for survival and propagation. In the setting of induced DNA damage, these cells must either respond with activation of repair pathways or undergo apoptosis. To negotiate this response, cell-cycle transitions are dependent upon checkpoint complexes that are tightly controlled through effectors such as P53. Accordingly, loss of P53 shifts the responsibility to other cell-cycle gatekeepers to ensure survival. Because up to 87% of GBMs have abnormalities in the p53 pathway, an alternate $G_2$ checkpoint is frequently activated in a p53-independent manner (3). A critical downstream mediator of this alternate checkpoint is the Wee1 kinase (4). The phosphorylated and stable Wee1 increases the level of inactivated phosphorylated-CDC2, leading to G2 phase checkpoint activation, thereby preventing damaged cells from entering into premature mitosis without repairing the DNA. Therefore, p53-deficient tumor cells treated with inhibitors of Wee1 are expected to be particularly susceptible to DNA damage induction due to genetic and pharmacologic loss of both the $G_1$ and $G_2$ checkpoints, respectively (5, 6).

AZD1775 is a potent and selective small-molecule inhibitor of the Wee1 kinase (half-maximal inhibitory concentration, 5.2 nmol/L in kinase screens; ref. 7) that inhibits phosphorylation of CDC2Tyr 15 and demonstrates suppression of Wee1 activity in various p53-deficient tumor cell lines (8). Through Wee1 inhibition, AZD1775 induces $G_2$ checkpoint escape and, thus, enhances the apoptotic effects of DNA-damaging agents and/or radiotherapy (5). In glioblastoma, Wee1 kinase is overexpressed and correlates inversely with overall survival,

[1]Ivy Brain Tumor Center, Barrow Neurological Institute, Phoenix, Arizona. [2]Karmanos Cancer Institute, Wayne State University, Detroit, Michigan. [3]The Translational Genomics Research Institute, Phoenix, Arizona. [4]Yale Cancer Center, Yale School of Medicine, New Haven, Connecticut.

**Note:** Supplementary data for this article are available at Clinical Cancer Research Online (http://clincancerres.aacrjournals.org/).

Prior presentation: The results were presented at the 52nd Annual Meeting of the American Society for Clinical Oncology, Chicago, IL, June 3–7, 2016.

**Corresponding Author:** Nader Sanai, Barrow Neurological Institute, 2910 N 3rd Avenue, Phoenix, AZ 85013. Phone: 602-406-3135; Fax: 602-406-6110; E-mail: nader.sanai@bnaneuro.net

**doi:** 10.1158/1078-0432.CCR-17-3348

Published OnlineFirst May 24, 2018; DOI: 10.1158/1078-0432.CCR-17-3348



## Translational Relevance

In this phase 0 trial, patients with recurrent glioblastoma were treated to the first-in-class Wee1-kinase inhibitor AZD1775 prior to planned reoperation. Animal studies have previously suggested that insufficient tumor–brain barrier penetration by the drug limits its therapeutic potential. In contrast, this study finds that unbound AZD1775, which represents the pharmacologically active fraction of the drug, reaches therapeutic concentrations within the contrast-enhancing component of the tumor. Furthermore, evidence of downstream target modulation was identified in a dose-dependent manner.

emphasizing its importance as a molecular target (9). With glioblastoma-derived cell lines, Wee1 kinase inhibitor treatment pushes cells through $G_2$ arrest, thereby inducing mitotic catastrophe (10). This strategy results in extensive cytotoxicity *in vitro*, as well as eradication of irradiated brain tumors in mice (9). Taken together, these preliminary findings suggest a role for AZD1775 as an adjuvant therapy for glioblastoma.

In neuro-oncology, challenges with blood–brain barrier penetration and limitations in the applicability of animal models to the human condition have hampered new drug development (11). Phase 0 clinical trials involve nontoxic drug doses administered for short periods to limited numbers of patients in order to obtain essential pharmacokinetic and pharmacodynamic data at the initial stage of the clinical trials process (12). To date, very few phase 0 studies for patients with glioblastoma have been published, as trials require meticulous timing of planned craniotomies in addition to customized assays for blood and tumor tissue analysis. Molecular profiling of tumors for patients with phase 0 glioblastoma may also yield insight to refine or accelerate drug development (13).

Although the characteristics of AZD1775 suggest it to be an effective molecule for blood–brain barrier penetration (14), preclinical data from a xenograft model of glioblastoma demonstrate extremely poor central nervous system (CNS) penetration and no evidence of pharmacodynamic effect (15). To resolve this controversy, we conducted a phase 0 study of AZD1775 in patients with first-recurrence glioblastoma. The primary objective of this study was to determine the plasma pharmacokinetics and brain tumor penetration of AZD1775 following a single oral dose in patients scheduled for re-resection of their recurrent glioblastoma. The pharmacokinetic results from this study determined if AZD1775 achieved pharmacologic concentration in brain tumors and if a once-daily dosing regimen maintained adequate drug exposure in plasma and tumor. Secondary objectives included evaluation of biomarkers corresponding to $G_2$ checkpoint escape, including indicators of apoptosis [cleaved caspase-3 (CC3) expression], mitotic escape (phosphohistone-3 expression), double-strand DNA damage (γH2AX expression), and molecular features of glioblastoma which may predispose to vulnerability to AZD1775.

## Patients and Methods

### Patient selection

All patients were ≥18 years old with a confirmed histologic diagnosis of glioblastoma (WHO grade IV). All patients previously had one prior resection of their tumor, followed by standard-of-care Stupp regimen temozolomide plus fractionated radiotherapy (1). Following radiographic and clinical evidence of disease progression, all patients were previously scheduled for clinically indicated surgical re-resection, had an Eastern Cooperative Oncology Group performance status of ≤2, and had adequate organ function.

### Study design and drug administration

This investigator-initiated, phase 0, open-label, nonrandomized study was conducted at the Barrow Neurological Institute in Phoenix, Arizona in partnership with Karmanos Cancer Institute and TGen. The study (ClinicalTrials.gov identifier: NCT02207010) received approval of the institutional medical ethical review board and was conducted in accordance with the Declaration of Helsinki and Good Clinical Practice. All patients were accrued at the Barrow Neurological Institute and gave written informed consent before inclusion in the study.

AZD1775 was supplied by AstraZeneca Pharmaceuticals under a collaborative agreement. Patients received a single dose of AZD1775 orally prior to surgical resection of their tumor. The doses under evaluation were 100, 200, and 400 mg. All doses have already been identified as safe monotherapy doses in a previously conducted phase I trial (16). In part 1 (dose-escalation) of our study, neurosurgical tumor resection was planned for 8 hours post drug administration at each of the three dose cohorts (Fig. 1A). For part 2 (time-escalation), neurosurgical resection was performed at 4, 8, or 24 hours following an oral dose of 400 (Fig. 1B–D). Blood sampling was performed alongside contrast-enhancing tumor samples collected intraoperatively.

### Safety and assessments

Demographic data and medical history were collected during screening. Physical examination, vital signs, and other safety assessments (Eastern Cooperative Oncology Group performance status, registration of concomitant medication, hematology, biochemistry, and urine analysis) were performed at baseline.

### Pharmacokinetic assessment

Sparse blood pharmacokinetic sampling was obtained from each patient. Blood samples for part 1 were collected at predosing, 8 hours (time of surgery), 12 hours, and 16 hours postdosing. Blood samples for part 2 with resection scheduled for 2 hours postdosing occurred at predosing, 2 hours (time of surgery), 8 hours, and 24 hours postdosing. Blood samples for part 2 with a resection scheduled for 24 hours postdosing occurred at predosing, 2, 8, and 24 (time of surgery) hours postdosing. At each time point, a 4-mL blood sample was collected into an EDTA tube, and plasma was separated by centrifugation (at 4°C, 1,500 × *g*, for 10 minutes). Plasma samples were stored at −80°C until analysis. One tumor sample from the contrast-enhancing region of the tumor was collected intraoperatively from each patient. Immediately after the collection, residual blood was washed off the tumor sample using ice-cold PBS, blot-dried on tissue paper, snap-frozen in liquid nitrogen, and stored at −80°C until analysis.

AZD1775 total concentrations in plasma and tumor samples were determined using a fully validated LC/MS-MS method as described previously by us (17). The fraction unbound in plasma or tumor tissue was determined by equilibrium dialysis

Published OnlineFirst May 24, 2018; DOI: 10.1158/1078-0432.CCR-17-3348



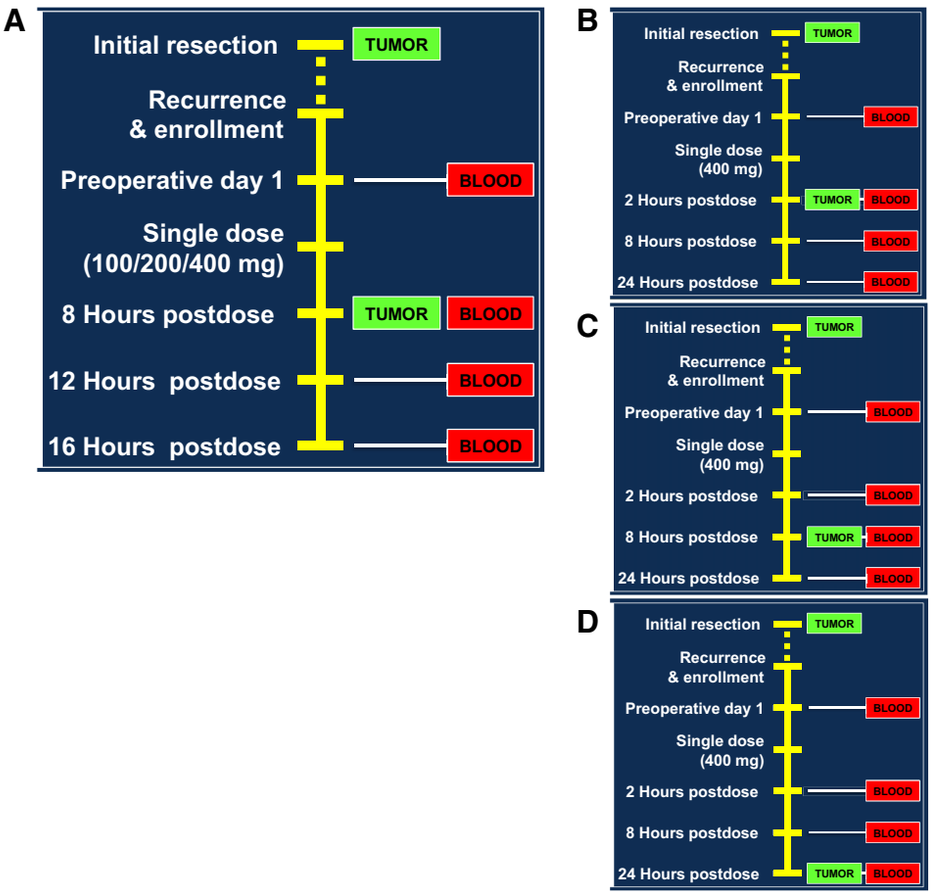


**Figure 1.**
Phase 0 study design composed of the dose-escalation arm (**A**) and the time-escalation arm (**B–D**).

(17). The unbound (i.e., pharmacologically active) drug concentration in plasma or tumor tissue was determined as the product of total drug concentration and fraction unbound.

### Pharmacodynamic assessment

One tumor sample (0.5 $cm^3$) per patient was collected from each patient and divided into two equal portions. Each portion was snap-frozen in liquid nitrogen immediately after collection and stored at −80°C until analysis. Formalin-fixed paraffin-embedded (FFPE) tissue from the patient's first tumor resection (at the time of initial diagnosis) was also accessed for this trial. Both archival FFPE tumor tissue and study specimens collected at the time of re-resection were assayed using standard IHC techniques to measure protein levels of double-stranded DNA damage (γH2AX), mitotic activity (phosphohistone-3, PH3), and programmed cell-death (CC3). Antibody conditions varied by target: CC3 (Cell Signaling Technology, D175, 1:50, overnight at 4°C), pH3 (Abcam, ab32107 1:100, overnight at 4°C), γH2AX (Millipore Sigma, 05-636 1:100 at room temperature for 1 hour). Images were obtained using the Panoramic Desktop Scanner (Caliper Life Sciences). Semi-quantitative IHC was performed using the Halo software system (Indica Labs).

To assess if the protein levels differ between nontreated primary and recurrent samples we analyzed four pairs of matched tissues from newly diagnosed and recurrent GBM samples. We performed IHC analysis with γH2AX, phosphohistone-3, and CC3 antibodies with the automated Bond Rx system (Leica Microsystems). Quantitative analysis was performed with the Aperio software (Leica Microsystems). Total numbers of positive cells were divided by total number of cells per field in five independent tumor-bearing fields. There was no significant difference in the number of γH2AX, phosphohistone-3, and CC3 positive cells between primary and recurrent samples.

### Genomic analysis

Genomic DNA from fresh frozen tissue specimen was isolated using DNAeasy Blood and Tissue Kit (Qiagen, #69504) according to manufacturer's protocol. Matched germline DNA for each patient was extracted and purified from the blood using a QIAamp DNA Blood Midi Kit/QIAamp Mini Kit from Qiagen.

Genomic tumor and normal DNAs (1.1 μg) for each sample were fragmented to a target size of 150 to 200 bp; 100 ng of fragmented product was run on TAE gel to verify fragmentation. The remaining 1 μg of fragmented DNA was prepared for sequencing on MiSeq using Agilent SureSelectXT Custom Kit for Sequencing as per the manufacturer's protocol. A custom MiSeq Kit for sequencing a selected panel of 25 genes [genes involved in $G_1$–S checkpoint pathway, Wee1, and 16 most frequently mutated genes in GBM (18); Supplementary Table S1] was designed through Agilent SureDesign for sequencing oligo design and used for library preparation.

DNA sequencing was performed on a MiSeq (Illumina) with 2 × 75-bp, paired-end reads according to the manufacturer's

instructions. For NGS data analysis, sequencing fastq files were aligned with BWA 0.6.2 to GRCh37.62 and the SAM output were converted to a sorted BAM file using SAMtools 0.1.18. BAM files were then processed through indel realignment, mark duplicates, and recalibration steps in this order with GATK 1.5. Comparative variant calling for NGS data was conducted with Seurat (19).

### Pharmacokinetic data analysis

Population pharmacokinetic analysis was performed to characterize total AZD1775 plasma concentration–time profiles and identify patient factors influencing the pharmacokinetics. The model was developed in two stages: structural model development followed by covariate model development. All analyses were performed with a first-order conditional estimation (FOCE) method with interaction using NONMEM program (version VII; ICON plc.). R version 2.6.2 was used for graphical diagnostics and covariate screen.

The structural model was built to fit total AZD1775 plasma concentration–time profiles after oral administration of a single dose (100, 200, and 400 mg) in 20 patients simultaneously. One- and two-compartment models with a first-order absorption and first-order elimination were tested. Mean population pharmacokinetic parameters, interindividual variability, and residual error (intraindividual variability) were assessed in the model. Interindividual variability of a pharmacokinetic parameter was expressed as an exponential function. Residual error was modeled with a combination method including an additive and a proportional part, each of which could be excluded if it was estimated to be negligible. The pharmacokinetic parameters for individual patients were obtained by *post hoc* Bayesian estimation.

A screen for potential statistically significant covariates was performed with a generalized additive model (GAM) using Xpose 4.0/R 2.6.2 software (Uppsala University, Uppsala, Sweden; ref. 20). The covariates as listed in Table 1, including sex, age, body size (i.e., weight, height, and BSA), serum albumin, liver function (i.e., alanine aminotransferase, aspartate aminotransferase, and total bilirubin), and kidney function (i.e., serum creatinine and creatinine clearance) were screened on all pharmacokinetic parameters in the structural model. Potentially statistically significant covariates selected from the GAM analysis were introduced into the covariate model as linear, exponential, or power functions according to the following discrimination criteria: (i) a decrease in the objective function value of greater than 3.875 ($P < 0.05$) during the forward covariate model building; (ii) an increase in the objective function value of greater than 10.828 ($P < 0.001$) during the stepwise backward model reduction; (iii) reduction of relative standard error of estimation; and (iv) reduction of interindividual variability of parameters.

**Table 1.** Patient demographics and clinical characteristics

| Characteristics | |
|---|---|
| Sex (male/female)[a] | 12/8 |
| Age (years) | 59 (28–81) |
| Weight (kg) | 79 (54–127) |
| Height (cm) | 172 (154–184) |
| Body surface area (BSA) ($m^2$) | 1.93 (1.52–2.43) |
| Alanine aminotransferase (IU/L) | 24 (14–133) |
| Aspartate aminotransferase (IU/L) | 16 (8–62) |
| Total bilirubin (mg/dL) | 0.5 (0.2–1.7) |
| Serum albumin (mg/dL) | 4.0 (2.1–4.6) |
| Serum creatinine (mg/dL) | 0.8 (0.6–1.0) |
| Glomerular filtration rate (mL/min)[b] | 98 (61–162) |

NOTE: Values are shown as median (range).
[a]Data indicate number of patients.
[b]Estimated by the Chronic Kidney Disease Epidemiology Collaboration (CKD-EPI) equation based on serum creatinine concentration (22).

The extent of drug penetration into the brain tumor was assessed by the total drug tumor-to-plasma partition coefficient ($K_p$) and unbound drug tumor-to-plasma partition coefficient ($K_{p,uu}$), which were estimated as the tumor to plasma concentration ratio of the total and unbound drug, respectively (21). It should be noted that because unbound drug concentration drives the *in vivo* pharmacological effect, the use of $K_{p,uu}$ as a measure of brain tumor penetration is more pharmacologically relevant.

### Pharmacodynamic data statistical analysis

Descriptive statistics and graphics (dot plots, with a horizontal line indicating the mean) were generated to summarize the Pharmacodynamic data. For each distribution of fold changes, the Normality assumption was examined using four tests: Shapiro–Wilk, Kolomogorov–Smirnov, Cramer–von Mises, and Anderson–Darling. If at least two of those four test statistics were significant at the 0.01 alpha level, then the distribution was considered non-normal.

Mean fold changes significantly different from 1.000 (indicating no change from the matched archival tissue) were of interest. For each distribution of fold changes, the mean fold change was tested vs. 1.000 using the one-sample *t* test (two-sided). For the few non-normal distributions, the nonparametric one-sample Wilcoxon signed-rank test (two-sided) was used instead, and that was specified where needed in the Results section.

As phase 0 studies are inherently exploratory, the nominal alpha level of 0.05 was used to interpret the test results without adjustment for test multiplicity (i.e., the multiple comparisons issue was not formally addressed). Two of these exploratory statistical testing results with $0.05 < P < 0.10$ were considered weakly significant. All statistical analyses of the pharmacodynamic data were performed using the Univariate Procedure in SAS software, Version 9.4.

## Results

### Patient population

Patient demographics and clinical characteristics are presented in Table 1. Twenty adult patients with glioblastoma received a single dose of AZD1775 prior to brain tumor resection and enrolled in either a dose-escalation arm (100, 200, or 400 mg) or a time-escalation arm at 400 mg (2, 8, or 24 hours), all without complications. AZD1775 was well-tolerated; no significant adverse effects were observed.

### Pharmacokinetics

Total AZD1775 plasma concentration–time profiles (Fig. 2A) following a single oral dose (100, 200, and 400 mg) in patients with glioblastoma were well-described by a one-compartment model with a first-order absorption rate constant ($K_a$) of 2.1 $hour^{-1}$, an apparent volume of distribution (V/F) of 1,500 L, and an apparent oral clearance (CL/F) of 160 L/hour. Glomerular filtration rate, estimated by the Chronic Kidney Disease Epidemiology Collaboration (CKD-EPI) equation

Published OnlineFirst May 24, 2018; DOI: 10.1158/1078-0432.CCR-17-3348



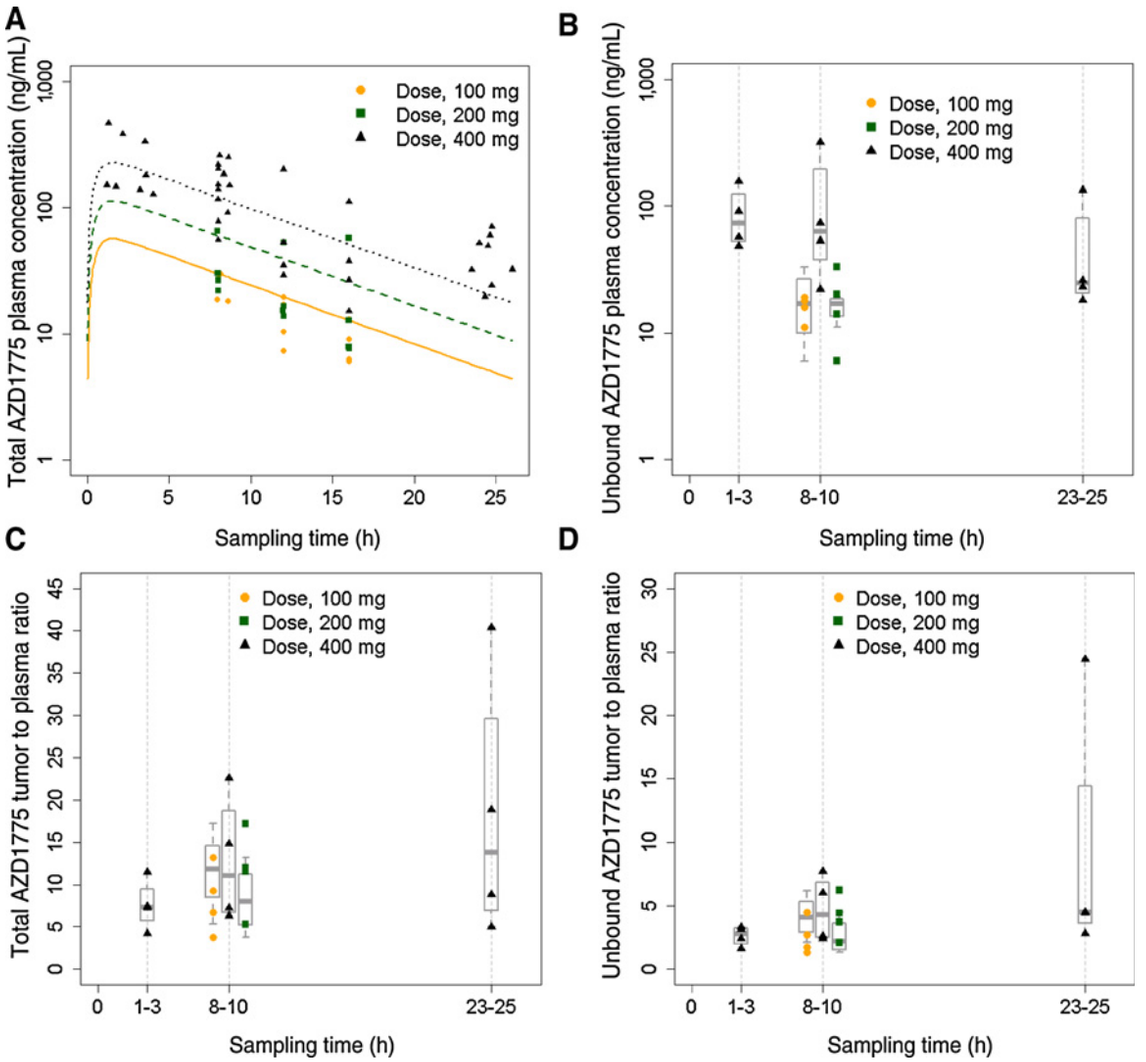


**Figure 2.**

AZD1775 plasma and tumor pharmacokinetics in patients with glioblastoma receiving a single oral dose. **A,** AZD1775 total plasma concentration–time profiles. Symbols represent observed concentrations; solid, dash, and dot lines represent pharmacokinetic profiles fitted by the final population pharmacokinetic model. **B,** Unbound AZD1775 tumor concentrations. **C,** AZD1775 total tumor-to-plasma concentration ratios. **D,** AZD1775 unbound tumor-to-plasma concentration ratios. Symbols represent observed data; boxplot represents 25th, 50th (median), and 75th percentiles of the observed data.

based on serum creatinine concentration (22), was identified as a significant covariate on the CL/F of AZD1775, explaining 17% of the interindividual variability of CL/F. Population pharmacokinetic parameters for the base and covariate models are summarized in Table 2. Goodness-of-fit plots for the final covariate model are presented in Supplementary Fig. S1.

The tumor exposure to unbound (pharmacologically active) AZD1775 as well as the extent of tumor penetration (assessed by $K_p$ and $K_{p,uu}$) are presented in Fig. 2B–D. The unbound AZD1775 tumor concentrations varied from 6 to 315 ng/g across three dose levels and three sampling time points, which were above the enzyme $IC_{50}$ (2.6 ng/mL) for inhibition of Wee1 activity. Of note, following a single oral dose of 400 mg, the mean unbound AZD1775 tumor concentration at 2 to 24 h (85 ng/g) exceeded the *in vitro* $IC_{50}$ (40 ng/mL) for the inhibition of Wee1 activity and induction of DNA damage as well as $G_2$ checkpoint escape in cell-based assays (https://ncats.nih.gov/files/AZD1775.pdf). The $K_p$ or $K_{p,uu}$ of AZD1775 were dose-independent following a single oral dose of 100, 200, and 400 mg, and time-independent at 2 to 24 hours post dosing indicating the achievement of brain equilibrium by 2 hours postdosing. Overall, across all tested dose levels and sampling time points, the $K_p$ varied up to 10.6-fold (range, 3.8–40.4; median, 9.1) and the $K_{p,uu}$ varied up to 18.8 fold (range, 1.3–24.4; median, 3.2) in 20 patients with glioblastoma.

### Pharmacodynamics

To determine whether AZD1775 modulated its target pathway, the molecular consequences of Wee1 pathway suppression were assessed, specifically, abrogation of $G_2$ arrest through quantification of histone-3 phosphorylation (PH3), DNA damage based on evidence of double-strand DNA breaks indicated γH2AX, and programmed cell death by expression

Published OnlineFirst May 24, 2018; DOI: 10.1158/1078-0432.CCR-17-3348



**Table 2.** Population pharmacokinetic parameters for total AZD1775, estimated from the base and final covariate models, data are expressed as estimates (%RSE)

| Parameter | Base model | Covariate model |
|---|---|---|
| OFV | −36.58 | −42.63 |
| $K_a$ ($h^{-1}$) | 2.00 (114) | 2.10 (111) |
| V/F (L) | 1,500 (16) | 1,500 (17) |
| CL/F (L/hour) | 160 (15) | 160[a] (14) |
| $B$[a] | | 1.7 (44) |
| IIV of $K_a$ (CV%) | 100 (310) | 100 (300) |
| IIV of V/F (CV%) | 28 (70) | 26 (91) |
| IIV of CL/F (CV%) | 48 (23) | 40 (36) |

Abbreviations: CL/F, apparent oral clearance; IIV, interindividual variability; $K_a$, first-order absorption rate constant; OFV, objective function value; RSE, relative standard error of estimation; V/F, apparent volume of distribution.
[a]$CL/F = A + B \times (GFR - 98)$, where A is the CL/F for a typical patient with glomerular filtration rate (GFR) of 98 mL/minute, and B represents the covariate effect of glomerular filtration rate.

of CC3. As described previously, primary and recurrent tumor was analyzed after dose- and time-dependent treatments of AZD1775 (Figs. 3 and 4).

To identify potential dose–response relationship with respect to AZD1775 inhibition of Wee1 functional endpoints in glioma, cohorts were assessed at 8 hours following 100, 200, or 400 mg of AZD1775 treatment. We observed double-stranded DNA damage, as measured by γH2AX, to be increased at the 200-mg dose cohort, as compared to matched archival tissue (Fig. 3A). At 8 hours, this increase was less dramatic for the 100- and 400-mg dose cohorts. Similar results were observed with cell-cycle abrogation, as measured by PH3 expression in Fig. 3B. Increased expression of PH3 was observed in the 200-mg dose cohort at 8 hours, as compared to matched archival tissue (Fig. 3B). Unlike γH2AX expression, however, PH3 expression was also substantially increased for the 400-mg dose cohort (Fig. 3B). Finally, the apoptotic marker CC3 increased most at the 200-mg dose cohort, as compared to matched archival tissue, although a modest increase was also observed in the 400-mg group, as well.

To assess potential time-dependency of AZD1775 pharmacodynamic effects on the Wee1 pathway, specimens were collected at 2-, 8-, and 24-hour time intervals following 400 mg AZD1775 dose. Additional data for other dose cohorts at 8 hours were also included in this analysis from the dose-escalating portion of the study. Interestingly, the 8-hour time interval provided the most variable expression of the pharmacodynamic endpoints.

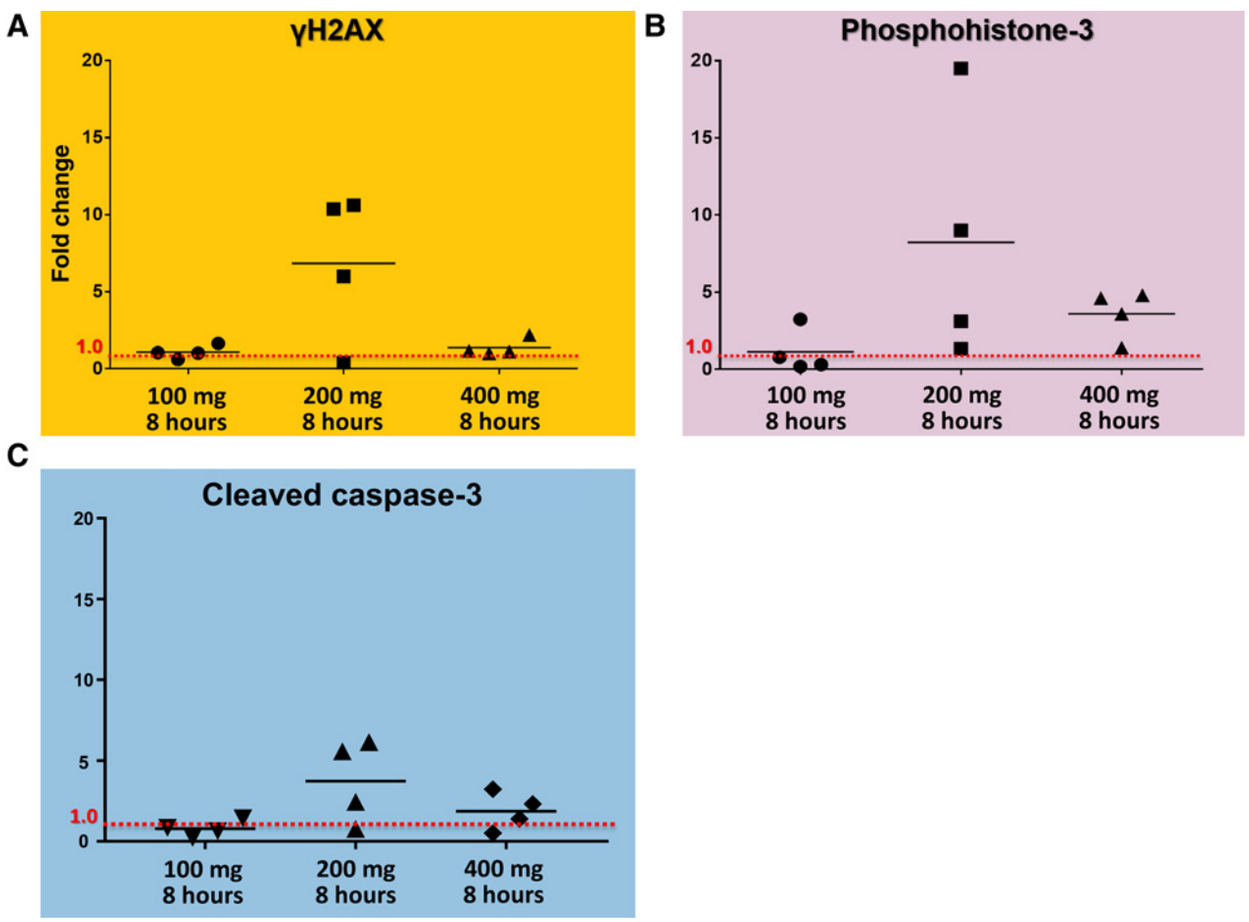


**Figure 3.**
In matched archival tissues following drug exposure, Wee1 pathway suppression was inferred by intensified double-strand DNA breakage (**A**), abrogation of $G_2$-arrest (**B**), and programmed cell death (**C**). Horizontal line marks the mean fold change.

Published OnlineFirst May 24, 2018; DOI: 10.1158/1078-0432.CCR-17-3348



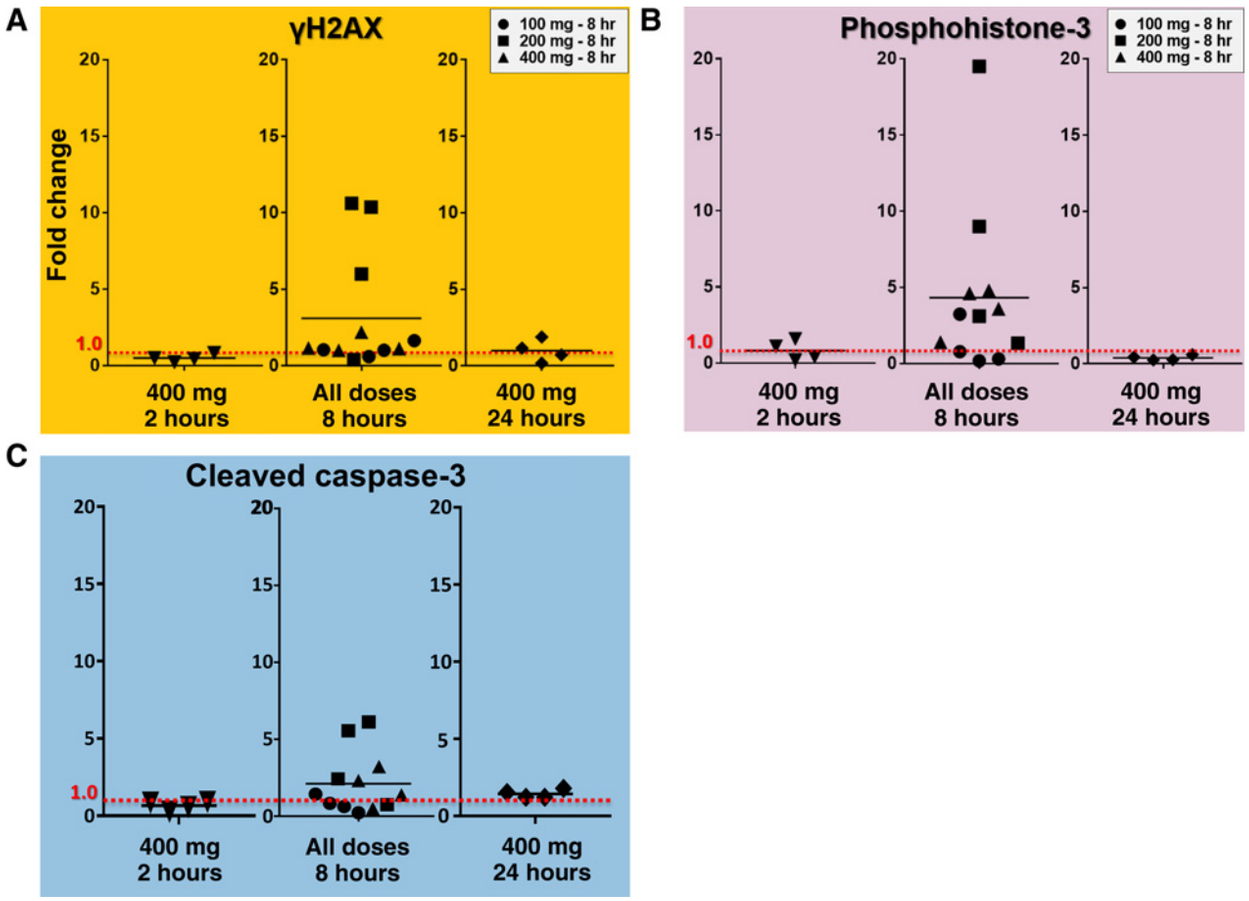


**Figure 4.**

In the time-escalation arm, γH2AX expression, phosphohistone-3 expression (PH3), and CC3 expression all demonstrated peak changes 8 hours following AZD1775 administration. Horizontal line marks the mean fold change.

Specifically, in the 8-hour time interval group combining all three dose cohorts ($n = 12$), there was a significant ($P = 0.0425$, by one-sample Wilcoxon signed-rank test) mean rise in γH2AX expression of +210.1% (Fig. 4A, range, −59.8% to +961.5%). Similarly, when all dose cohorts are assessed together at the 8-hour time interval ($n = 12$), PH3 expression increased significantly, as well (Fig. 4B, $P = 0.0210$, by one-sample Wilcoxon signed-rank test). Finally, when all dose cohorts were assessed together at the 8-hour time interval ($n = 12$), CC3 expression increased ($P = 0.0727$) by a mean of +112.2% (Fig. 4C, range, −76.8% to +513.6%).

### Targeted sequencing

Genes involved in $G_1$–S checkpoint regulation, Wee1, and 16 genes frequently mutated in glioblastoma were sequenced (Supplementary Table S1). Aberrations in 11 genes out of panel of selected 25 genes were observed across 20 patients (Supplementary Table S2). In five of the 20 patients, inactivating mutations in TP53 were found, six with aberrations in EGFR (although two were in untranslated regions), and six had mutations in PTEN. One case showed mutation in IDH1. None of the cases had mutations in Wee1; mutations in other genes were detected less frequently. No consistent associations between any of the pharmacokinetic or pharmacodynamic endpoints and these molecular events were uncovered.

## Discussion

Our findings provide molecular evidence for proof-of-target inhibition by AZD1775, as well as plasma and tumor pharmacokinetic data in patients with glioblastoma. Taken together, these results will serve as the foundation for subsequent combinatorial agent studies including AZD1775.

Sufficient penetration of anticancer drugs into brain tumors is a prerequisite for effective treatment of glioblastoma. AZD1775 shows good brain tumor penetration in patients with first-recurrence glioblastoma, achieving pharmacologically relevant tumor concentrations. Our data support further clinical development of AZD1775 for treating recurrent glioblastoma. Notably, our findings differ from preclinical studies using orthotopic glioblastoma xenograft mouse models, which previously reported very limited distribution of AZD1775 in mouse normal brain and tumor tissues (15). Although the exact mechanism(s) underlying this discrepancy remains to be determined, the observed inter-species variability in AZD1775 brain tumor penetration underscores the value of early, prospective

Published OnlineFirst May 24, 2018; DOI: 10.1158/1078-0432.CCR-17-3348



evaluation of drug penetration into human brain and brain tumors to inform decision making regarding future clinical development. Multiple factors could have contributed to these divergent results, including diminished net efflux clearance of AZD1775 at human blood–brain tumor barrier due to the acidic tumor microenvironment, variation in the transporter expression profiles at human and rodent blood–brain tumor barrier, and inherent variation in blood–brain tumor barrier integrity (17). Regardless of mechanism(s), our phase 0 findings emphasize the importance of "humanizing" preclinical models for targeted inhibitors in glioblastoma.

One limitation of our pharmacokinetic study, however, was the lack of noncontrast-enhancing glioblastoma tissue in our tissue analysis. The contrast-enhancing regions of the tumors, which were used for the assessment of AZD1775 brain tumor penetration in our study, often presents disrupted, "leaky" blood–brain tumor barrier. The drug (including AZD1775) would be expected to have less penetration into non-contrast-enhancing glioblastoma tissue. Future glioblastoma drug penetration studies would benefit from analyzing both the contrast- and noncontrast-enhancing regions of the tumor. It should be mentioned, however, that neither of these regions have an intact blood–brain barrier around the tumor's neovasculature (23) and thus, the measurements of drug penetration into these regions do not represent drug penetration into "normal" brain tissue. Further studies employing *in vivo* microdialysis technique may provide detailed pharmacokinetic information on drug penetration into both normal brain and tumor tissue

Beyond effective tumor penetration, our findings also detail a range of molecular profiles associated with subtherapeutic AZD1775 administration in patients with recurrent glioblastoma. Disruption of tightly controlled cell-cycle safeguards through Wee1 inhibition can lead to premature entry into mitosis and, ultimately, mitotic catastrophe. Importantly, evidence for these events were observed in patient-derived specimens. Specifically, at the 8-hour posttreatment interval, double-stranded DNA damage increased over eightfold, cell-cycling increased over threefold, and programmed cell death also increased threefold (Figs. 3 and 4). Although these findings do not demonstrate direct molecular effects from Wee1 inhibition, they are consistent with checkpoint disruption.

Interestingly, observed pharmacodynamic effects were most prominent at the 200 mg dose level and less evident at 400 mg. The lack of dose–response relationship may be attributed to a combination of multiple mechanisms, including large interindividual variability in the drug tumor pentration/exposure, small sample size, and complex feedback loops regulating Wee1 inhibition. In addition, because of the tested pharmacodynamic endpoints are not exclusively driven by Wee1 inhibition, it is possible that other tumor-intrinsic factors influenced their response to the drug. Nevertheless, our data suggests that a 200-mg dose regimen may be sufficient for the pharmacodynamic effects in future clinical studies. Our study highlights the importance of an initial phase 0 evaluation of pharmacodynamic effects in aiding dose selection for the subsequent therapeutic trials.

In summary, our findings refute previous preclinical data and show excellent brain tumor penetration for AZD1775 in humans, providing the first evidence of clinical biological activity in human glioblastoma, and confirmed the utility of phase 0 trials as part of an accelerated paradigm for early drug development in patients with brain tumors. Although the phase 0 clinical trial paradigm is not new in oncology, our application of this strategy for patients with recurrent glioblastoma underscores its suitability for an expanded role in studying human glioma biology and fast-tracking targeted inhibitor drug development. Given the inherent limitations of animal modeling in predicting therapeutic benefit for human gliomas, there appears to be an important role for carefully conceived, pharmacokinetically and pharmacodynamically driven, early phase clinical trials in neuro-oncology. Surveys of genomic profiles relevant to the drug under study (gene and pathway targets, transporter genes, etc.) further raise the value of phase 0 trials in glioblastoma to accelerate development of new treatments for this disease.

## Disclosure of Potential Conflicts of Interest

P.M. LoRusso is a consultant/advisory board member for ivePrime, Roche-Genentech, and Takeda. No potential conflicts of interest were disclosed by the other authors.

## Authors' Contributions

**Conception and design:** N. Sanai, J. Li, L.K. Heilbrun, M.E. Berens, P.M. LoRusso

**Development of methodology:** N. Sanai, J. Li, J. Boerner, K. Stark, J. Wu, M.E. Berens, P.M. LoRusso

**Acquisition of data (provided animals, acquired and managed patients, provided facilities, etc.):** N. Sanai, J. Li, J. Boerner, K. Stark, J. Wu, A. Derogatis, H.D. Dhruv, M.E. Berens

**Analysis and interpretation of data (e.g., statistical analysis, biostatistics, computational analysis):** N. Sanai, J. Li, J. Boerner, J. Wu, S. Kim, A. Derogatis, S. Mehta, H.D. Dhruv, L.K. Heilbrun, M.E. Berens

**Writing, review, and/or revision of the manuscript:** N. Sanai, J. Li, J. Boerner, S. Kim, S. Mehta, H.D. Dhruv, L.K. Heilbrun, P.M. LoRusso

**Administrative, technical, or material support (i.e., reporting or organizing data, constructing databases):** N. Sanai, J. Wu

**Study supervision:** N. Sanai, J. Li, S. Mehta

## Acknowledgments

This work was supported in part by the American Society for Clinical Oncology, the Ben & Catherine Ivy Foundation, and the United States Public Health Service Cancer Center Support Grant (P30 CA022453). We thank AstraZeneca for providing the study drug (AZD1775) for this trial and we are indebted to the patients who enrolled in this study.

The costs of publication of this article were defrayed in part by the payment of page charges. This article must therefore be hereby marked *advertisement* in accordance with 18 U.S.C. Section 1734 solely to indicate this fact.

Received November 9, 2017; revised January 12, 2018; accepted March 2, 2018; published first May 24, 2018.

## References

1. Stupp R, Mason WP, van den Bent MJ, Weller M, Fisher B, Taphoorn MJ, et al. Radiotherapy plus concomitant and adjuvant temozolomide for glioblastoma. N Engl J Med 2005;352:987–96.

2. Weller M, Cloughesy T, Perry JR, Wick W. Standards of care for treatment of recurrent glioblastoma–are we there yet? Neuro Oncol 2013;15:4–27.

3. The Cancer Genome Atlas Research Network. Comprehensive genomic characterization defines human glioblastoma genes and core pathways. Nature 2008;455:1061–8.
4. Russell P, Nurse P. Negative regulation of mitosis by wee1+, a gene encoding a protein kinase homolog. Cell 1987;49:559–67.
5. Leijen S, Beijnen JH, Schellens JH. Abrogation of the G2 checkpoint by inhibition of Wee-1 kinase results in sensitization of p53-deficient tumor cells to DNA-damaging agents. Curr Clin Pharmacol 2010;5:186–91.
6. Wang Y, Decker SJ, Sebolt-Leopold J. Knockdown of Chk1, Wee1 and Myt1 by RNA interference abrogates G2 checkpoint and induces apoptosis. Cancer Biol Ther 2004;3:305–13.
7. Hirai H, Arai T, Okada M, Nishibata T, Kobayashi M, Sakai N, et al. MK-1775, a small molecule Wee1 inhibitor, enhances anti-tumor efficacy of various DNA-damaging agents, including 5-fluorouracil. Cancer Biol Ther 2010;9:514–22.
8. Rajeshkumar NV, De Oliveira E, Ottenhof N, Watters J, Brooks D, Demuth T, et al. MK-1775, a potent Wee1 inhibitor, synergizes with gemcitabine to achieve tumor regressions, selectively in p53-deficient pancreatic cancer xenografts. Clin Cancer Res 2011;17:2799–806.
9. Mir SE, De Witt Hamer PC, Krawczyk PM, Balaj L, Claes A, Niers JM, et al. In silico analysis of kinase expression identifies WEE1 as a gatekeeper against mitotic catastrophe in glioblastoma. Cancer Cell 2010;18:244–57.
10. De Witt Hamer PC, Mir SE, Noske D, Van Noorden CJ, Wurdinger T. WEE1 kinase targeting combined with DNA-damaging cancer therapy catalyzes mitotic catastrophe. Clin Cancer Res 2011;17:4200–7.
11. Oberoi RK, Parrish KE, Sio TT, Mittapalli RK, Elmquist WF, Sarkaria JN. Strategies to improve delivery of anticancer drugs across the blood-brain barrier to treat glioblastoma. Neuro Oncol 2016;18:27–36.
12. Kummar S, Rubinstein L, Kinders R, Parchment RE, Gutierrez ME, Murgo AJ, et al. Phase 0 clinical trials: conceptions and misconceptions. Cancer J 2008;14:133–7.
13. Reifenberger G, Wirsching HG, Knobbe-Thomsen CB, Weller M. Advances in the molecular genetics of gliomas—implications for classification and therapy. Nat Rev Clin Oncol 2017;14:434–52.
14. Hirai H, Iwasawa Y, Okada M, Arai T, Nishibata T, Kobayashi M, et al. Small-molecule inhibition of Wee1 kinase by MK-1775 selectively sensitizes p53-deficient tumor cells to DNA-damaging agents. Mol Cancer Ther 2009;8:2992–3000.
15. Pokorny JL, Calligaris D, Gupta SK, Iyekegbe DO Jr, Mueller D, Bakken KK, et al. The efficacy of the Wee1 inhibitor MK-1775 combined with temozolomide is limited by heterogeneous distribution across the blood-brain barrier in glioblastoma. Clin Cancer Res 2015;21:1916–24.
16. Do K, Wilsker D, Ji J, Zlott J, Freshwater T, Kinders RJ, et al. Phase I study of single-agent AZD1775 (MK-1775), a Wee1 kinase inhibitor, in patients with refractory solid tumors. J Clin Oncol 2015;33:3409–15.
17. Wu J, Sanai N, Bao X, LoRusso P, Li J. An aqueous normal-phase chromatography coupled with tandem mass spectrometry method for determining unbound brain-to-plasma concentration ratio of AZD1775, a Wee1 kinase inhibitor, in patients with glioblastoma. J Chromatogr B Analyt Technol Biomed Life Sci 2016;1028:25–32.
18. Brennan CW, Verhaak RG, McKenna A, Campos B, Noushmehr H, Salama SR, et al. The somatic genomic landscape of glioblastoma. Cell 2013;155:462–77.
19. Christoforides A, Carpten JD, Weiss GJ, Demeure MJ, Von Hoff DD, Craig DW. Identification of somatic mutations in cancer through Bayesian-based analysis of sequenced genome pairs. BMC Genomics 2013;14:302.
20. Jonsson EN, Karlsson MO. Xpose–an S-PLUS based population pharmacokinetic/pharmacodynamic model building aid for NONMEM. Comput Methods Programs Biomed 1999;58:51–64.
21. Hammarlund-Udenaes M, Friden M, Syvanen S, Gupta A. On the rate and extent of drug delivery to the brain. Pharm Res 2008;25:1737–50.
22. Levey AS, Stevens LA, Schmid CH, Zhang YL, Castro AF III, Feldman HI, et al. A new equation to estimate glomerular filtration rate. Ann Intern Med 2009;150:604–12.
23. Rong Y, Durden DL, Van Meir EG, Brat DJ. 'Pseudopalisading' necrosis in glioblastoma: a familiar morphologic feature that links vascular pathology, hypoxia, and angiogenesis. J Neuropathol Exp Neurol 2006;65:529–39.

AACR American Association for Cancer Research

Clinical Cancer Research

# Phase 0 Trial of AZD1775 in First-Recurrence Glioblastoma Patients

Nader Sanai, Jing Li, Julie Boerner, et al.

*Clin Cancer Res* 2018;24:3820-3828. Published OnlineFirst May 24, 2018.